Acta Oceanol. Sin., 2021, Vol. 40, No. 6, P. 111–128
https://doi.org/10.1007/s13131-021-1780-8
http://www.aosocean.com
E-mail: ocean2@hyxb.org.cn

Living coccolithophores in the western Pacific Ocean with mesoscale eddies

Danyue Huang[1, 2], Haijiao Liu[1, 2], Jun Sun[2, 3]*, Yuqiu Wei[1, 2], Liuyang Li[1, 2], Guicheng Zhang[2, 3], Laxman Pujari[2, 3]

[1] Institute of Marine Science and Technology, Shandong University, Qingdao 266200, China

[2] Research Centre for Indian Ocean Ecosystem, Tianjin University of Science and Technology, Tianjin 300457, China

[3] Tianjin Key Laboratory of Marine Resources and Chemistry, Tianjin University of Science and Technology, Tianjin 300457, China

Received 25 December 2019; accepted 27 April 2020

Abstract

Living coccolithophores (LCs) are regarded as a group of calcifiers and play important roles in global carbon cycle. This study used microscopic observations of LCs in the western Pacific Ocean to investigate their community structure and biodiversity, especially to test whether local physical traits (mesoscale eddies) could explain their biogeographic distributions during autumn of 2017. The coccolithophore calcite inventory based on carbon-volume transformation was estimated in this study. A total of 28 taxa of coccospheres and 19 types of coccoliths were identified from 161 samples. *Gephyrocapsa oceanica* was the most predominant species in all the coccolithophore community, followed by *Florisphaera profunda*, *Emiliania huxleyi*, *Umbilicosphaera sibogae*, *Gladiolithus flabellatus* and *Umbellosphaera tenuis*. The abundance of coccospheres and coccoliths ranged from 0 to 26.8×10^3 cells/L and from 0 to 138.5×10^3 coccoliths/L, averaged at 4.2×10^3 cells/L and 10.9×10^3 coccoliths/L, respectively. This study indicated that coccolithophore community in the survey area can be clustered into four groups. Three ecological niches of coccolithophores were characterized by their vertical profiles and multivariate statistical analysis. Coccolithophore abundance and species composition were remarkably different among warm-eddy region, *G. oceanica* dominated warm-eddy region, while *F. profunda* dominated warm-eddy and none-eddy region. The average values of estimated particulate inorganic carbon, particulate organic carbon were 0.197 μg/L and 0.140 μg/L, respectively. The current field study widened the dataset of coccolithophores in western Pacific Ocean.

Key words: living coccolithophores, western Pacific Ocean, carbon cycle, mesoscale eddy, warm eddy, cold eddy

Citation: Huang Danyue, Liu Haijiao, Sun Jun, Wei Yuqiu, Li Liuyang, Zhang Guicheng, Pujari Laxman. 2021. Living coccolithophores in the western Pacific Ocean with mesoscale eddies. Acta Oceanologica Sinica, 40(6): 111–128, doi: 10.1007/s13131-021-1780-8

1 Introduction

Living coccolithophores (LCs) are an important function group of phytoplankton in the ocean (Taylor et al., 2017). Through double carbon pump mechanisms (biological pump and carbonate counter pump), they regulate the ocean-atmosphere CO_2 fluxes and play essential roles in global carbon cycle (Sun, 2007). The relative intensity of calcification and photosynthesis performed by coccolithophores influences carbon cycling between atmosphere and ocean (Shutler et al., 2013; Perrin et al., 2016). Rain ratio, which termed as calcium carbonate to organic carbon of sinking biogenic particles, acts as a key factor in carbon cycle (Hutchins, 2011). Coccolithophores, as one of the major primary producer in marine ecosystem, contribute to about 15% of marine phytoplankton biomass (Berger, 1976) and up to 60% of the bulk pelagic calcite deposited on the ocean floors (Honjo, 1996). They also affect global sulfur cycle by producing dimethylsulfoniopropionate (Taylor et al., 2017). In addition, coccolithophores can scatter light efficiently using their highly optically refractive coccoliths (Balch, 2018), thus coccolithophore bloom can be easily observed from space by satellite remote sensing. Recently, being potentially sensitive to climate change especially to ocean acidification, coccolithophores have attracted significant attention globally (Doney et al., 2009).

Previous research on coccolithophore community structure emphasizes spatial distribution (Okada and Honjo, 1973; Honjo and Okada, 1974; Okada and McIntyre, 1977; Reid, 1980; Hagino et al., 2000, 2005; Saavedra-Pellitero et al., 2011, 2014; López-Fuerte et al., 2015) and factors controlling in global oceans. As one of the largest oligotrophic areas, however, the western Pacific Ocean (WPO) particularly with reference to LCs has received far less attention than other oceans. To date, there are rare records about the diversity and distribution of LCs in the WPO. Meanwhile, research found that environmental factors and ocean current may affect LCs. For instance, Okada and Honjo (1975) found that nitrogen deficiency may lead to diverse forms and degrees of malformation in coccolithophores. And research in eastern Indian Ocean presented that abundant coccolithophores occurred in accordance with the presence of Wyrtki jets (Liu et al., 2018), further confirming that environmental factors

Foundation item: The National Natural Science Foundation of China under contract Nos 41876134, 41676112 and 41276124; the University Innovation Team Training Program for Tianjin under contract No. TD12-5003; the Tianjin 131 Innovation Team Program under contract No. 20180314; the Changjiang Scholar Program of Chinese Ministry of Education under contract No. T2014253.
*Corresponding author, E-mail: phytoplankton@163.com

and ocean current may affect the abundance of coccolithophores. To enhance the appreciation of the importance of various forms of LCs, similar investigation should be conducted in regional scale with higher spatial resolution in the WPO, considering the significant contributions of LCs to primary production and calcite production.

The WPO is considered as oligotrophic and unproductive area (Messié and Radenac, 2006), which is dominated by diverse oceanic gyres. This study presumed that the spatio-temporal variability in LCs might be closely related to the annual variations of circulations or mesoscale eddies in the WPO. This study thereafter compared the LCs communities and associated environmental variables in autumn of 2017 to address the following questions: (1) what are the diversity, abundance and distribution of LCs in the WPO? (2) how do major environmental variables influence their abundances? (3) what are different distributions and ecological preference of LCs as a result of the circulations or mesoscale eddies in the WPO? and (4) what is the significance of LCs in carbon cycle?

This study aimed to explore the physical-biological coupling effects of mesoscale eddies on LC communities by means of polarizing microscope approach and quantify contribution of LCs in WPO carbon cycle.

2 Materials and methods

2.1 *Oceanographic settings*

A multidisciplinary investigation was carried out in the Western Pacific Warm Pool (WPWP) (2°–18°N, 126°–130°E) from October 25 to November 12, autumn of 2017. Twenty-seven stations were investigated as shown in Fig.1. As the warmest ocean spanning from the WPO to the eastern Indian Ocean, the WPWP is a typically oligotrophic area characterized by high temperature and low primary productivity (Messié and Radenac, 2006). And its interaction with Western Boundary Current (WBC) has a significant role in shaping complex circulation systems on both regional and global scales (Hu et al., 2016). Figure merged sea surface height and geostrophic sea water velocity was used to present the existence and conditions of mesoscale eddies (Fig. 2). The geostrophic currents of mesoscale features during this investigation were obtained from the Copernicus Marine Environment Monitoring Service database (http://marine.copernicus.eu/). Blocked by the Philippine islands at 14°–15°N, the North Equatorial Current (NEC) bifurcates into the northward Kuroshio Current (KC) and southward Mindanao Current (MC) (Hu et al., 2015). A characteristic feature is the presence of two semi-permanent eddies at the overturning zone of Mindanao Current and New Guinea Coastal Current (NGCC) (Zhai et al., 2013). One is the Mindanao Eddy (ME) which present at northern side with cyclonic circulation, the other is the Halmahera Eddy (HE) which present at the southern side with cyclonic circulation. The North Equatorial Counter Current (NECC) forms the boundary between them at 5°N (Arruda and Nof, 2003). In addition, another anticyclonic circulation is observed at around 15°N. In general, except for Halmahera warm eddy, there are two cold eddies with cyclonic circulation where current-driving upwellings occurred. Previous research found that phytoplankton blooms can occasionally occur as a result of upwellings (Chen et al., 2018, 2017).

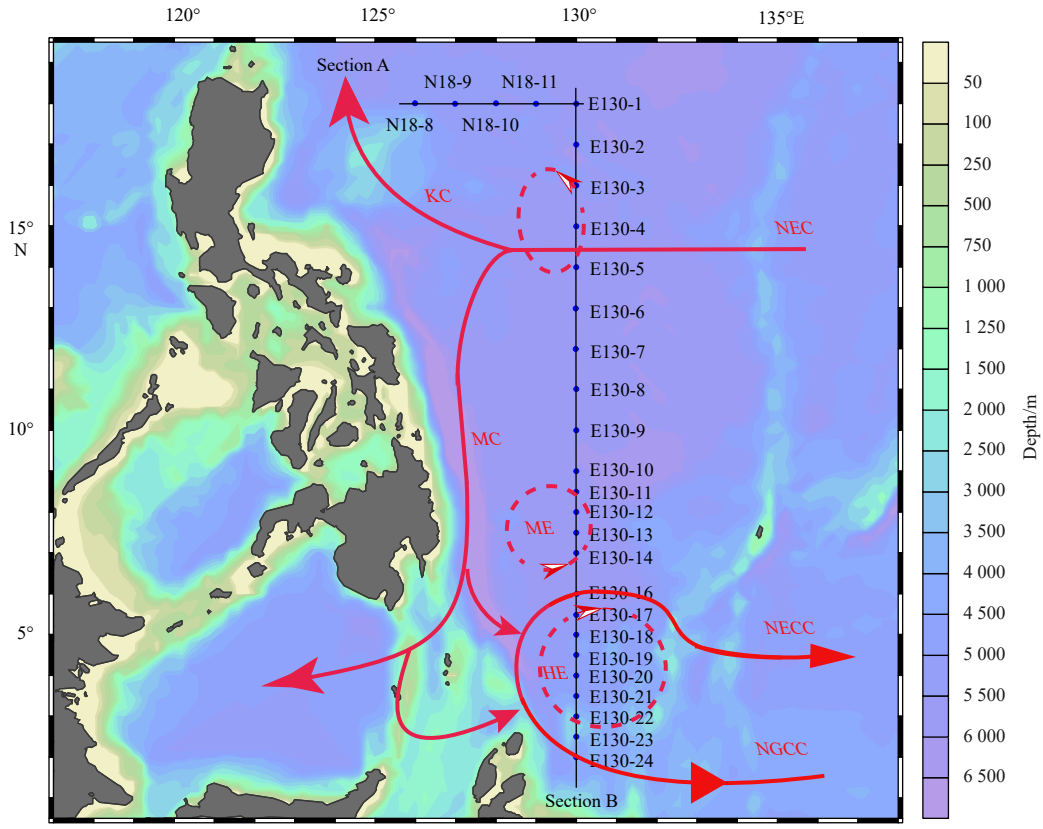

Fig. 1. The sampling stations and surface circulation in the western Pacific Ocean. NEC, North Equatorial Current; KC, Kuroshio Current; MC, Mindanao Current; NECC, North Equatorial Counter Current; NGCC, New Guinea Coastal Current; ME, the Mindanao Eddy; HE, the Halmahera Eddy.

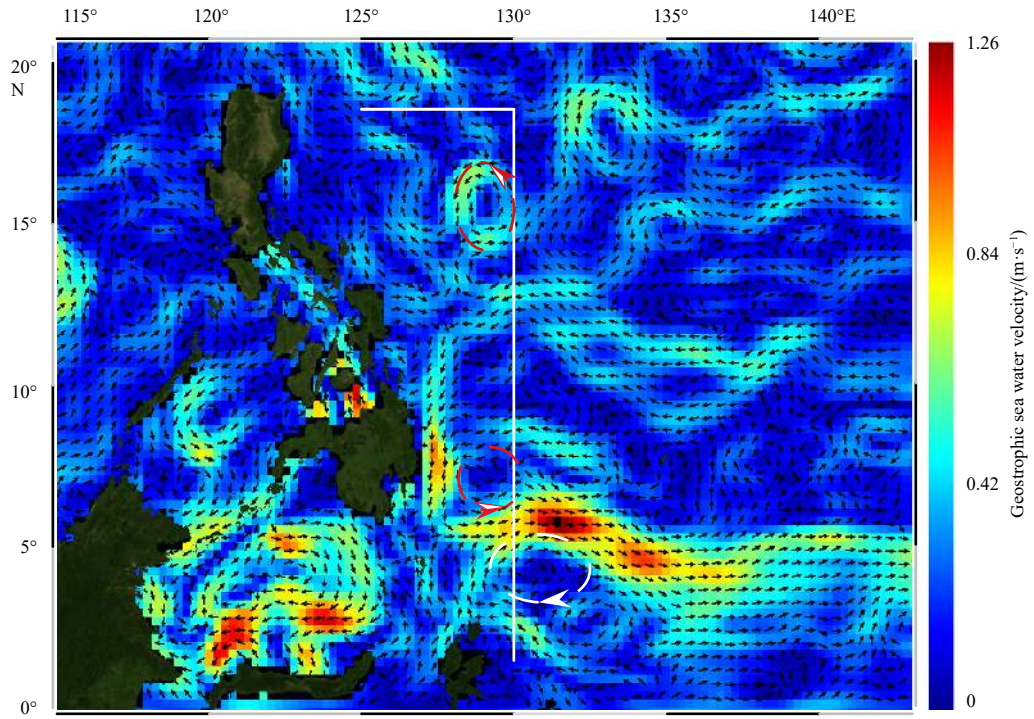

Fig. 2. Geostrophic sea water velocity (m/s) and mesoscale-eddies in the western Pacific Ocean in November 2017 (http://marine.copernicus.eu/). The anticyclonic eddies are marked with white circles, while cyclonic eddies are marked with red circles. The white lines represent two sampling sections.

2.2 *Sampling collection*

A total of 161 seawater samples were obtained from 27 stations (Fig. 1). Two sections (Section A and Section B) were designed to explore coccolithophore abundance and diversity. At each station, water samples were collected at seven depths within the upper 200 m by multiple rosette sampler equipped with a Seabird CTD (Conductivity, Temperature and Depth) equipment. Temperature, salinity and depth data were all recorded *in situ* at the same time. Furthermore, LCs samples (1 L) were fixed with 1% buffered formaldehyde and stored at room temperature in darkness until later laboratory analysis. For nutrient analysis, seawater samples were filtered through 0.45 μm cellulose acetate membrane filters and then immediately refrigerated at –20°C. In addition, seawater samples were filtered through GF/F filters (Whatman, 25 mm) and wrapped in aluminum foil at –20°C for chlorophyll *a* (Chl *a*) analysis.

2.3 *Sampling analysis*

After returning to the laboratory, LCs samples (1 000 mL per-sample) were filtered through mixed cellulose ester membrane (25 mm in diameter, 0.8 μm in pore size) under a filtration vacuum of less than 0.02 MPa. After drying in plastic Petri-dishes at room temperature, the filters were mounted on glass slides with neutral balsam for polarizing microscope (Motic, BA300POL) examination (Sun et al., 2014). About 200–400 fields were observed under 1 000× magnification with more than 300 coccoliths or 100 coccospheres being identified and counted per filter (Bollmann et al., 2002). The coccolithophore identification is principally referred to Yang et al. (2003), Jordan et al. (2004), Frada et al. (2010), and the specialized website http://www.mikrotax.org/Nannotax3/index.php?dir=Coccolithophores.

Nutrient concentrations (including phosphate, silicate, nitrate, nitrite, and ammonium) were determined by a Technicon AA3 Auto-Analyzer (Bran + Luebbe) according to the classical colorimetric methods. Dissolved inorganic phosphorus (DIP) and silicate (DSi) were measured using spectrophotometry with standard molybdic acids and Murphy Riley molybdenum blue reagents according to Brzezinski and Nelson (1986) and Karl and Tien (1992), respectively. Dissolved inorganic nitrogen (DIN) was analyzed using the copper-cadmium column reduction method (Pai et al., 2001; Guo et al., 2014).

Filters for Chl *a* analysis were placed into 20 mL glass tubes, the pigments were then extracted by 5 mL 90% acetone, and quickly stored in the dark at 4°C for 24 h. Finally, the Chl *a* content were measured using a CE Turner Designs Fluorometer (Welschmeyer, 1994; Liu et al., 2015; Wei et al., 2019).

2.4 *Estimation of particulate inorganic carbon (PIC) and particulate organic carbon (POC)*

Coccolith volume was estimated by means of the specific shape constant (K_S) and maximum diameter (L, μm) (m, pg according to carbon) (Young and Ziveri, 2000; Yang and Wei, 2003). And then it was converted into calcite quotas (PIC) by the formula (Young and Ziveri, 2000):

$$m = 2.7 \times K_s \times L^3, \quad (1)$$

where 2.7 is the density of calcite (pg /μm³, according to carbon).The calcite mass for coccosphere was estimated by multiplying that of a single coccolith by the number of coccoliths in one coccosphere. The estimate number of coccoliths in one coccosphere referred to Yang and Wei (2003). Due to the irregular

shapes and insufficient Scanning Electron Microscope records in species *Gladiolithus flabellatus* and *Oolithotus antillarum*, this study did not statistically cover their calcite mass. The carbon biomass of all coccolithophore species identified in this study was recorded by O'Brien et al. (2013). Considering that cytoplasm dimensions in coccolithophore cells were rarely published in previous study, observations of coccosphere dimensions were more available. Based on their work, they assigned an idealized shape to each species such as sphere, then evaluated the biovolume of coccolithophore species (V, μm^3) from standard geometric models (Sun and Liu, 2003) and finally converted biovolume into carbon biomass (pg/cell, according to carbon) (Eppley et al., 1970).

$$\lg C = -0.642 + 0.089 \times \lg V. \tag{2}$$

2.5 *Data processing*

The abundance of coccoliths and coccospheres was calculated as the following equation by Sun et al. (2011):

$$A = \frac{a \times S \times 1\,000}{N \times b \times s}, \tag{3}$$

where A is the abundance of the species (cells/L or coccoliths/L); a is the number of total cells of a species in the whole viewing field of a filter; N is the number of fields counted in each filter; b is the volume of the water filtered (mL); 1 000 is for unite conversion; S is the effective filtration area; and s is the area per field under 1 000× magnification.

The relative abundance (P) and dominance index (Y) of coccoliths and coccospheres were calculated as the following methodology:

$$P_i = \frac{n_i}{N}, \tag{4}$$

$$Y = \frac{n_i}{N} f_i, \tag{5}$$

where N is the total number of individuals counted in the collected samples; n_i is the number of cells of the species i; and f_i is the occurrence frequency of the species i in each sample (Sun et al., 2003).

Alpha-diversity indices including Chao1 richness estimator, Shannon diversity indices, and Simpson diversity index were calculated with R v3.6.1 software (R Core Team, 2013).

Species ranked in the top ten dominances were considered as the dominant species in the WPO. Horizontal and vertical distributions of LCs abundance were depicted by the Ocean Data View (5.1.2). Box-whisker plots were prepared by the Golden Software Grapher 10.3.825 (LLC, USA) (https://support.goldensoftware.com/hc/en-us/categories/115000653847-Grapher). Coccosphere cluster and multi-dimensional scaling (MDS) analysis were carried out using PRIMER 6.0 to reveal spatial patterns in the community structure. To avoid the effects of rare species on the community (Wei et al., 2017), species with a dominance index (Y) less than 0.02% were excluded in cluster and MDS analysis. In order to study the relationship between LC abundance and environmental factors (temperature, salinity, nitrate, nitrite, ammonium, phosphate, silicate and sampling depth), Canonical Correspondence Analysis (CCA) (ter Braak, 1986) was applied using CANOCO for Window 4.5 and SPSS 21.

3 Results

3.1 *Hydrography*

The temperature in the surveyed stations ranged from 11.16°C to 30.19°C, averaged at (25.10±5.14)°C, while salinity varied from 33.38 to 35.24, with an average of (33.46±0.43). Surface distributions of temperature and salinity are shown in Fig. 3. The 28°C isotherm was regarded as the WPWP boundary, thus all stations were surveyed within the WPWP region. High temperature and low salinity were observed at the surface water around the equator (Fig. 4). Mixed layer depth (MLD) was defined as the depth where the temperature difference was over than 0.5°C relative to surface waters (Painter et al., 2010). Thermocline depth was taken where the temperature gradient >0.05°C/m (Jiang et al., 2016). Average MLD was around 50–80 m and thermocline depth ranged from 50 m to 100 m through the current transect of WPO (Fig. A1). And the halocline was slightly shallower than thermocline due to the great injection of fresh water induced by annual precipitation (Li et al., 1998). The range and mean values of nutrient concentrations are shown in Table 1. The concentration of nutrients peaked in eddy area because of the upwelling by the ME and transportation from shelf area (Fig.4). Due to the KC influence, phosphate concentration was relatively low at Section A. However, N/P ratio in most areas were less than 14 at Section B.

3.2 *The taxonomic composition of LCs*

A total of 29 species of coccolithophores were identified, consisting of 28 taxa of coccospheres and 19 types of coccoliths. *Gephyrocapsa oceanica*, *Florisphaera profunda*, *Emiliania huxleyi*, *Umbilicosphaera sibogae*, *G. flabellatus* and *Umbellosphaera tenuis* were more abundant in the WPO (Table 2). Coccosphere assemblages were dominated by *G. oceanica* and *F. profunda*, together representing 60% of total abundance. It is worth mentioning that *E. huxleyi*, which was the predominant species in coastal waters, only composed 8% of total abundance. *Gephyrocapsa oceanica* was also overwhelmingly dominant in coccolith, with a frequency of 93.46% and relative abundance of 86.47%. Other types of coccolith occurred at low abundance (<4%).

The abundance of coccospheres and coccoliths ranged from 0 to 26.8×10^3 cells/L and 0 to 138.5×10^3 coccoliths/L, with average values of 4.2×10^3 cells/L and 10.9×10^3 coccoliths/L, respectively (Fig. A2). The most predominant coccolith was *G. oceanica* and its abundance ranged from 0 to 131.3×10^3 coccoliths/L, averaged at 9.4×10^3 coccoliths/L. The most predominant coccosphere *G. oceanica* was ranged as 0–24.2×10^3 cells/L, with a mean value of 1.9×10^3 cells/L.

3.3 *The distributions of LCs*

The surface distribution of dominant coccoliths (Fig. A3) and coccospheres (Fig. 5) showed similar trend. High abundance zones were found around HE and ME. Abundance were relatively low in the water column north of 9°N. For coccolith, two dominant species *G. oceanica* and *E. huxleyi* showed high abundance near the equator. *Umbellosphaera irregularis*, *U. tenuis* and *D. tubifera* were primarily concentrated near two cyclonic eddies, the ME and another cold eddy at around 15°N. Coccospheres, primarily including *G. oceanica* (84.2%), were recorded with the highest abundance of 26.8×10^3 cells/L at Station E130-22 (3°N, 130°E). High abundance of *E. huxleyi*, *C. cristatus* and *U. sibogae* were observed at Section A.

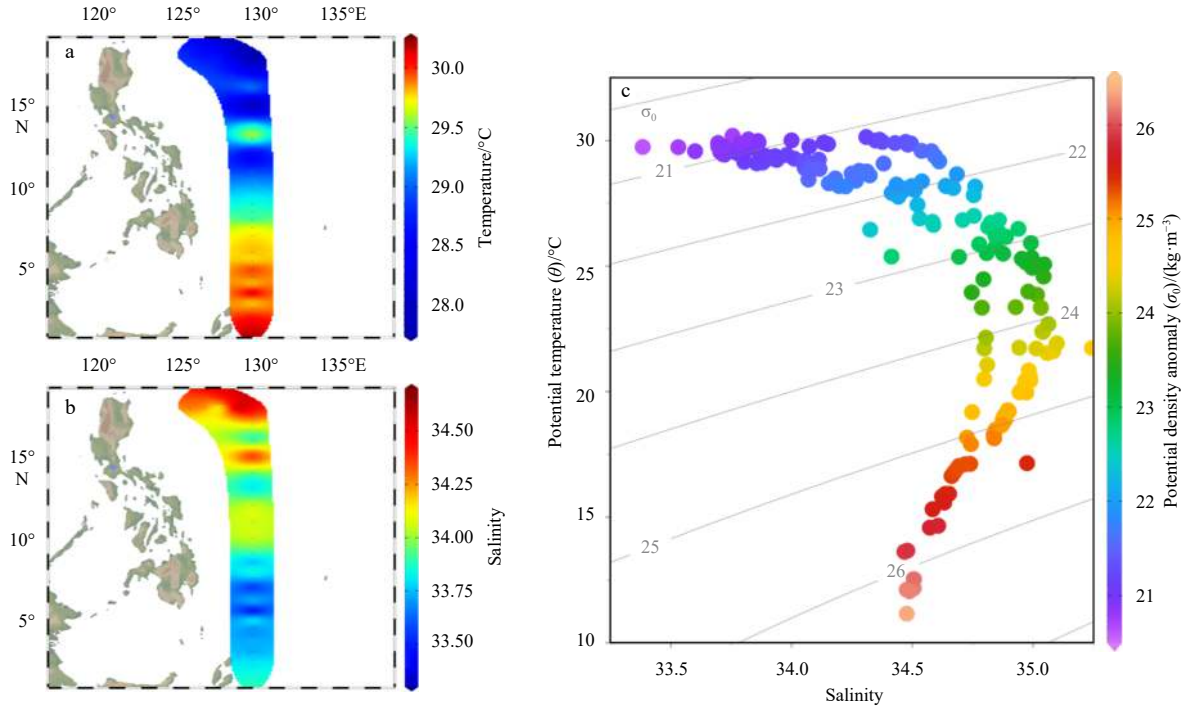

Fig. 3. Surface distribution of temperature and salinity in the surveyed area. a. Temperature, b. salinity, and c. temperature-salinity (*T*-*S*) diagram.

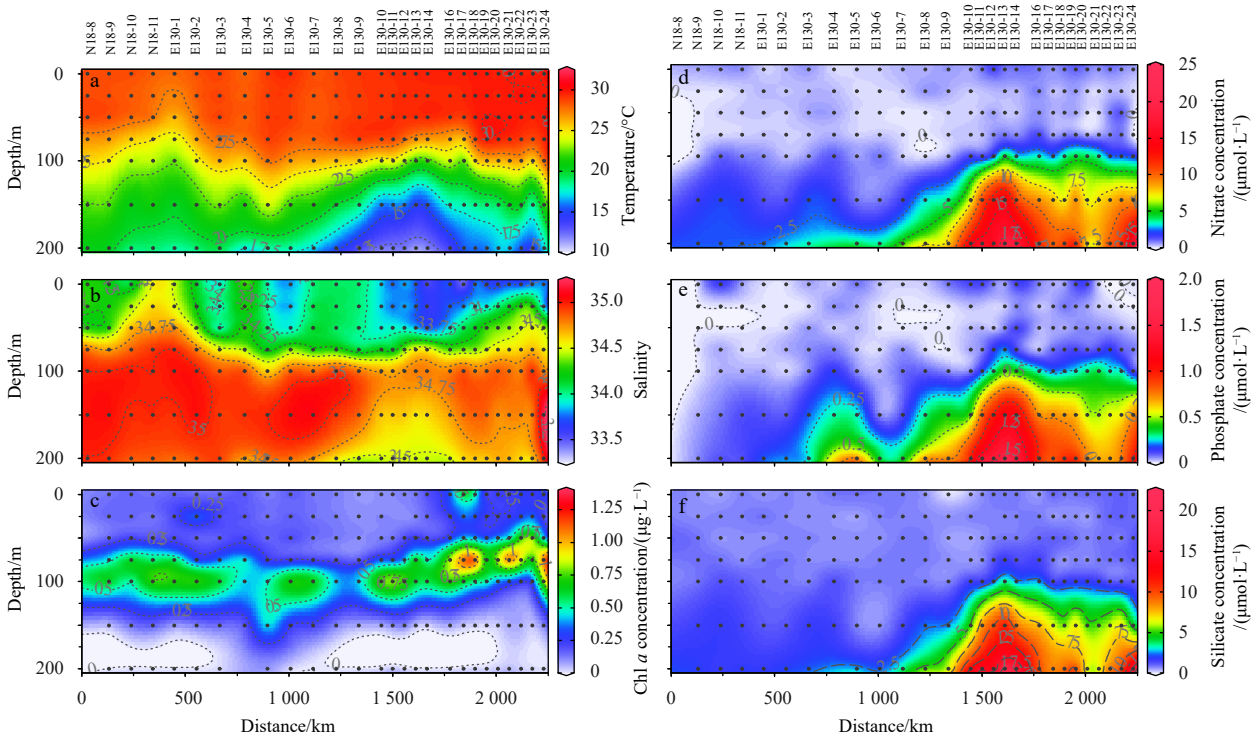

Fig. 4. Vertical distribution of temperature, salinity, chlorophyll *a* concentration, nitrate concentration, phosphate concentration, silicate concentration in the surveyed area.

Vertically, the dominant coccoliths were concentrated to 25–100 m. Most of them increased with depth in 0–75 m and then decreased to the bottom (200 m). Otherwise, the abundance of *C. cristatus* decreased with depth throughout the water column. Abrupt abundance increases of coccoliths and coccospheres in vertical variation presented patchy or "bull's eye" distribution (Figs 6, A4). Nutrient enrichment makes for the survival and growth of coccolithophores around eddies (Baumann et al., 2005). For coccosphere species, *G. oceanica* and *E. huxleyi* dominated the upper photic zone, *U. sibogae* and *G. flabellatus* mostly occurred at

Table 1. Range and mean values of nutrient concentrations

Parameter	Range	Mean
Nitrate concentration/(μmol·L^{-1})	0.01–22.87	2.78±4.39
Nitrite concentration/(μmol·L^{-1})	0.03–0.36	0.11±0.06
Phosphate concentration/(μmol·L^{-1})	0–1.80	0.23±0.35
Silicate concentration/(μmol·L^{-1})	0.45–21.74	2.52±3.64
Ammonium concentration/(μmol·L^{-1})	0–2.86	0.51±0.54

Table 2. Occurrence frequency, relative abundance and dominance degree of dominant coccoliths and coccospheres

Taxon	Average abundance/ (coccoliths·L^{-1}) or (cells·L^{-1})	Frequency (f_i)/%	Relative abundance (P_i)/%	Dominance index (Y)
Coccolith dominant species				
Gephyrocapsa oceanica	9 418.0	93.46	86.47	0.808 2
Emiliania huxleyi	359.5	41.18	3.30	0.013 6
Umbellosphaera tenuis	356.0	29.41	3.31	0.009 7
Umbilicosphaera sibogae	243.8	22.22	2.24	0.005 0
Ceratolithus cristatus	0.153 1	18.95	1.41	0.002 7
Coccolithophore dominant species				
Gephyrocapsa oceanica	1 945.0	62.89	45.78	0.287 9
Florisphaera profunda	659.1	45.28	15.51	0.070 2
Emiliania huxleyi	374.5	52.20	8.81	0.046 0
Umbilicosphaera sibogae	332.4	31.45	7.82	0.024 6
Gladiolithus flabellatus	138.5	22.01	3.26	0.007 2
Umbellosphaera tenuis	0.114 7	25.16	2.70	0.006 8
Umbellosphaera irregularis	116.4	16.98	2.74	0.004 7
Algirosphaera robusta	82.4	21.38	1.94	0.004 1
Discosphaera tubifera	72.2	16.35	1.70	0.002 8
Oolithotus antillarum	100.0	10.06	2.35	0.002 4

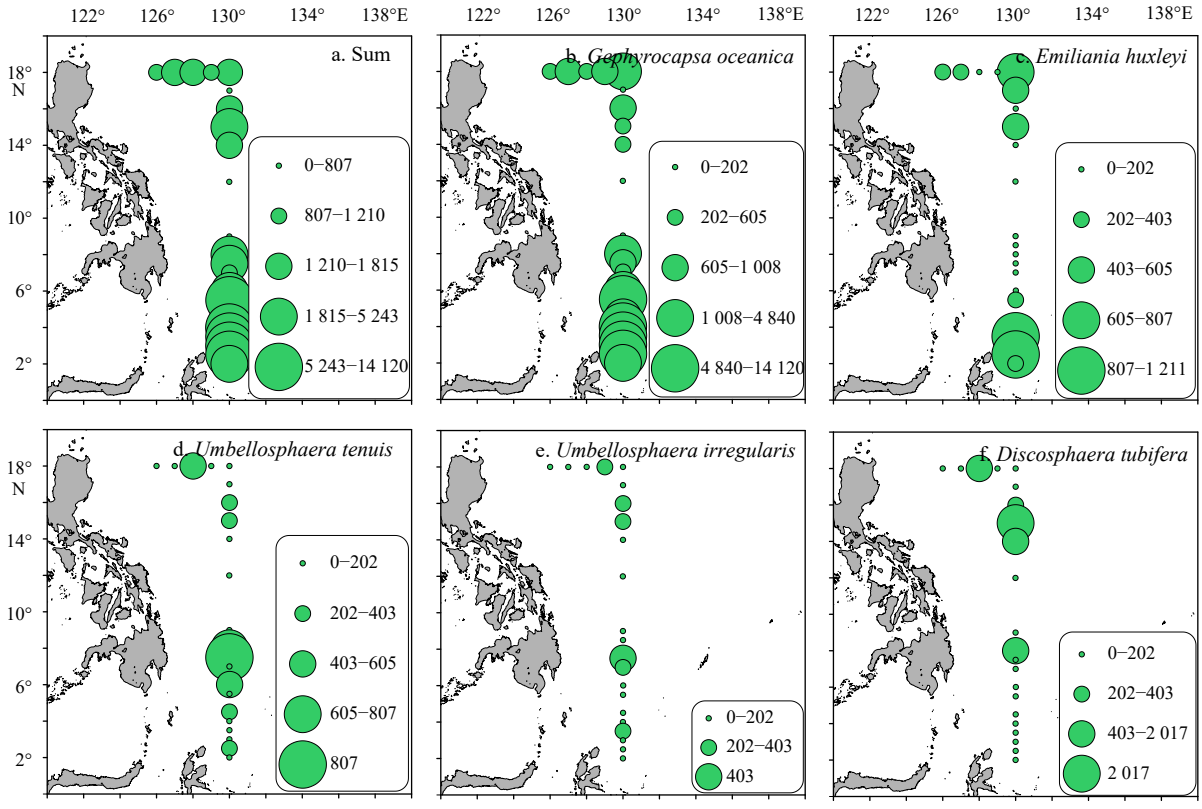

Fig. 5. Surface distribution of dominant coccospheres (cells/L) in the surveyed area.

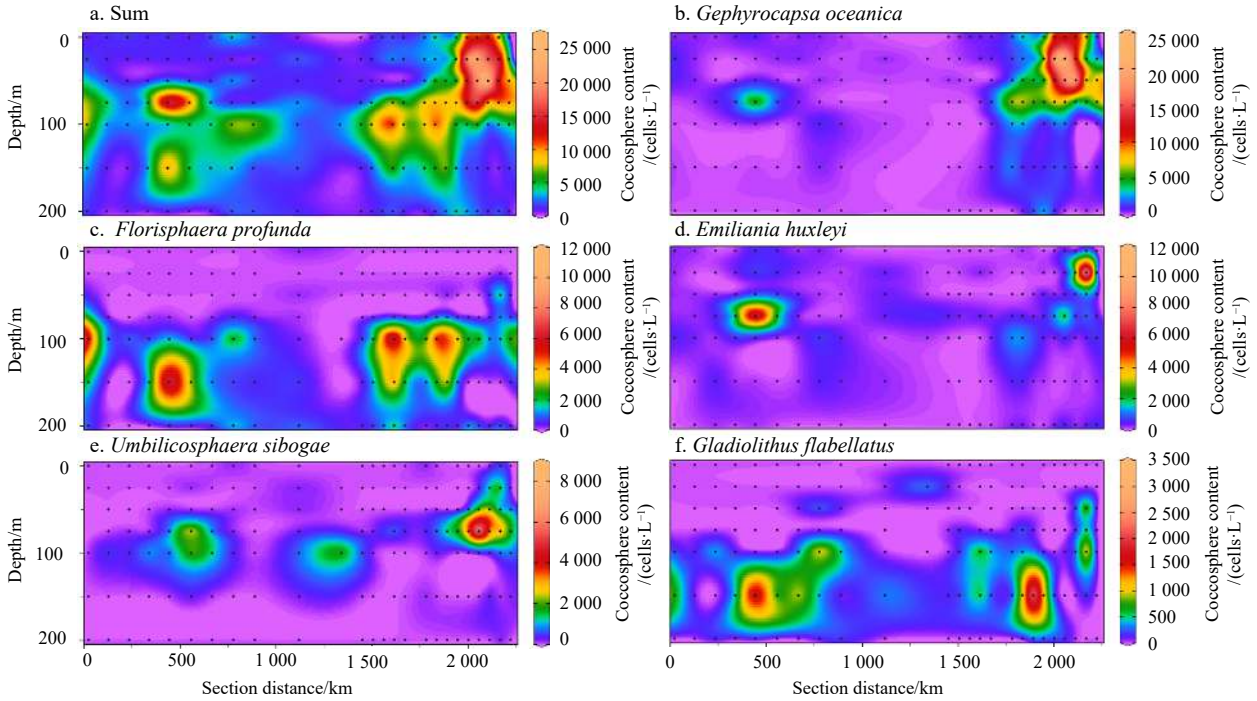

Fig. 6. The vertical distribution of dominant coccosphere along the section of the surveyed area.

the bottom of photic zone and *F. profunda* concentrated near the deep chlorophyll maximum (DCM) layer (Figs A5 and A6). Therefore, consistent with previous observations by Hagino et al. (2000), coccolithophores occupied different ecological niches according to their environmental preference. The ratios between coccospheres and free coccoliths along the water column increase from the surface to 100 m layer, this is because that coccospheres disintegrated into coccoliths in upper 100 m, resulting in the increase of coccoliths. However, the ratios decreased after the 100 m depth owing to the dissolution of coccoliths (Fig. 7).

3.4 *Estimate of PIC, POC and PIC/POC*

The average values of PIC, POC and PIC/POC were (0.197±0.280) μg/L (according to corbon), (0.140±0.232) μg/L (according to corbon) and (1.809±1.210), respectively. Biogenic PIC was mainly contributed by *G. oceanica* (30.24%), *U. sibogae* (26.12%) and *O. fragilis* (18.51%) (Fig. 8a). Due to the large biovolume, *U. sibogae* dominated POC and accounted for 48.79% of total (Fig. 8b). The surface distributions and depth-integrated patterns of PIC and POC are shown in Fig. 9. Surface distributions of both PIC and POC showed high values at Station E130-4 (15°N, 130°E). Within this station, *O. fragilis* contributed to 47.0% of PIC and *U. sibogae* contributed to approximately 28.3% of POC. The surface distribution of POC was in accordance with the abundance of coccospheres. The surface and depth-integrated pattern of PIC and POC showed similar trend near equator, with high values occurring at HE.

3.5 *Cluster and multi-dimensional scaling analysis*

Cluster and MDS analysis for coccospheres were carried out at 75 m layer (Figs 10a and b) where α-diversity indices were higher than other layers (Table A1). With top ten dominants from 22 stations as biological factors, LCs community could be clustered into four groups according to different environmental

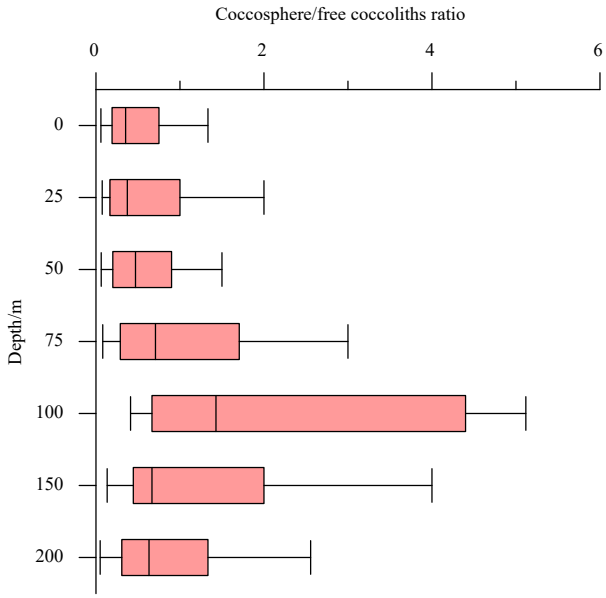

Fig. 7. The ratio of coccosphere to free coccoliths in upper ocean column in the surveyed area.

drivers: Groups A–D. MDS stress values (0.12) lesser than 0.2 give a useful ordination picture, particularly at the lower end of this range (Cox and Cox, 1992; Clarke et al., 2014; Liu et al., 2018). Group A contained ten stations around HE except Station E130-1. At these stations, elevated nutrients transported by MC and NECC from shelf area facilitated coccolithophore growth. *Gephyrocapsa oceanica* was the most dominant species in these stations. In addition, *U. sibogae* was abundant in the upper 75 m at HE. *Florisphaera profunda* was commonly distributed around mesoscale eddies. Whereas, high abundance of *G. flabellatus* and

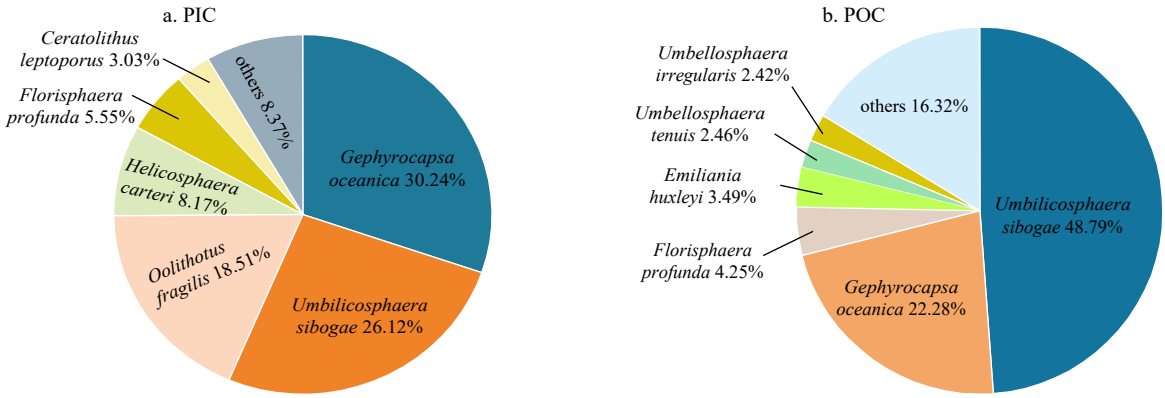

Fig. 8. Contribution of dominant coccolithophores to particulate inorganic carbon (PIC) and particulate organic carbon (POC).

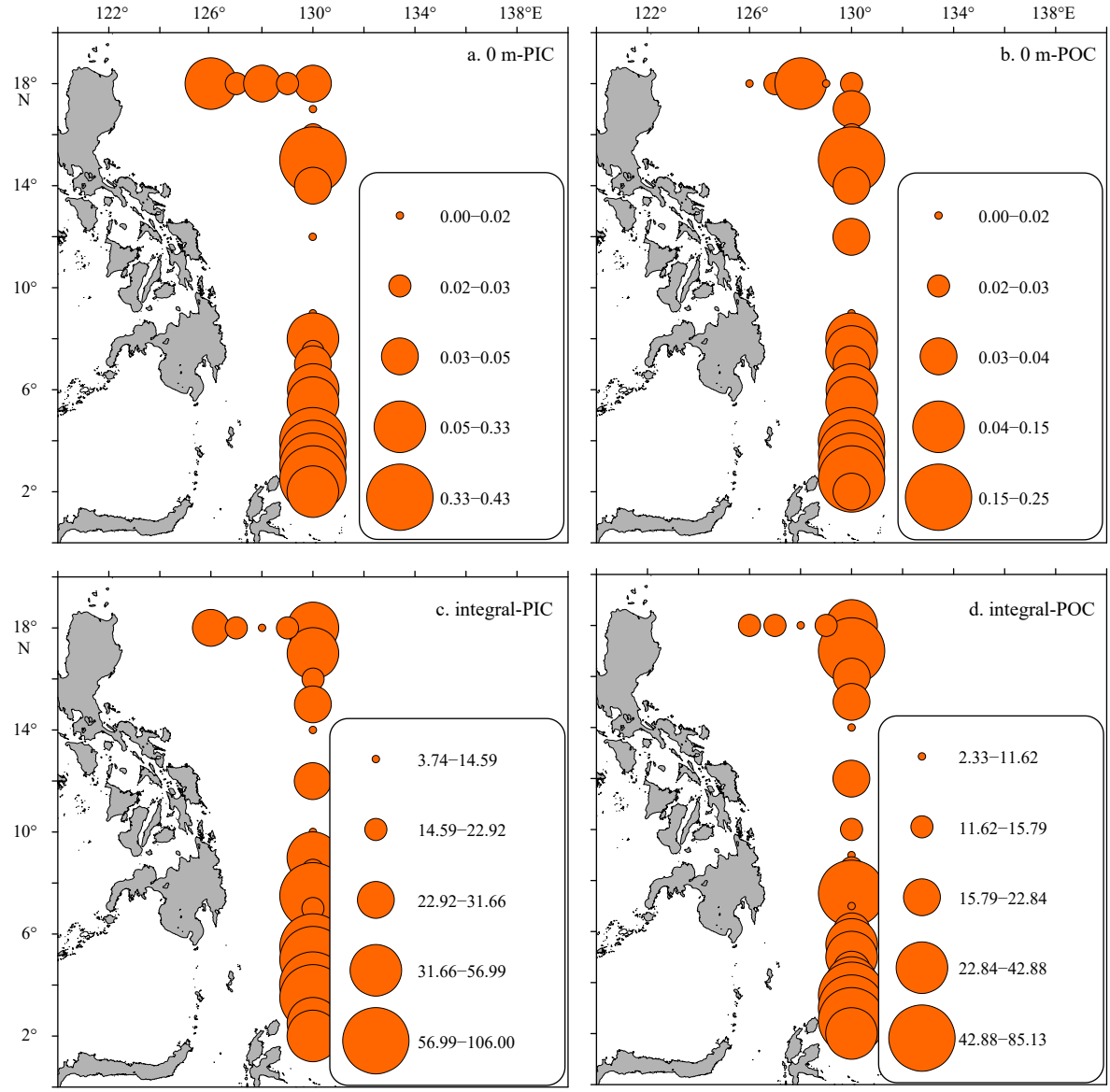

Fig. 9. Surface distribution and depth-integrated patterns of coccolith particulate inorganic carbon (PIC, μg/L) and coccolithophore particulate organic carbon (POC, μg/L).

A. robusta were observed at the bottom of photic zone with low light and high nutrients. Group B covered six stations around two cyclonic eddies, where abundant *F. profunda* were lifted by upwelling from the bottom. *Oolithotus antillarum* and *U. irregularis* preferred to distribute near cold eddies (Fig. 11). Group C consisted of several stations, which were not influenced by meso-

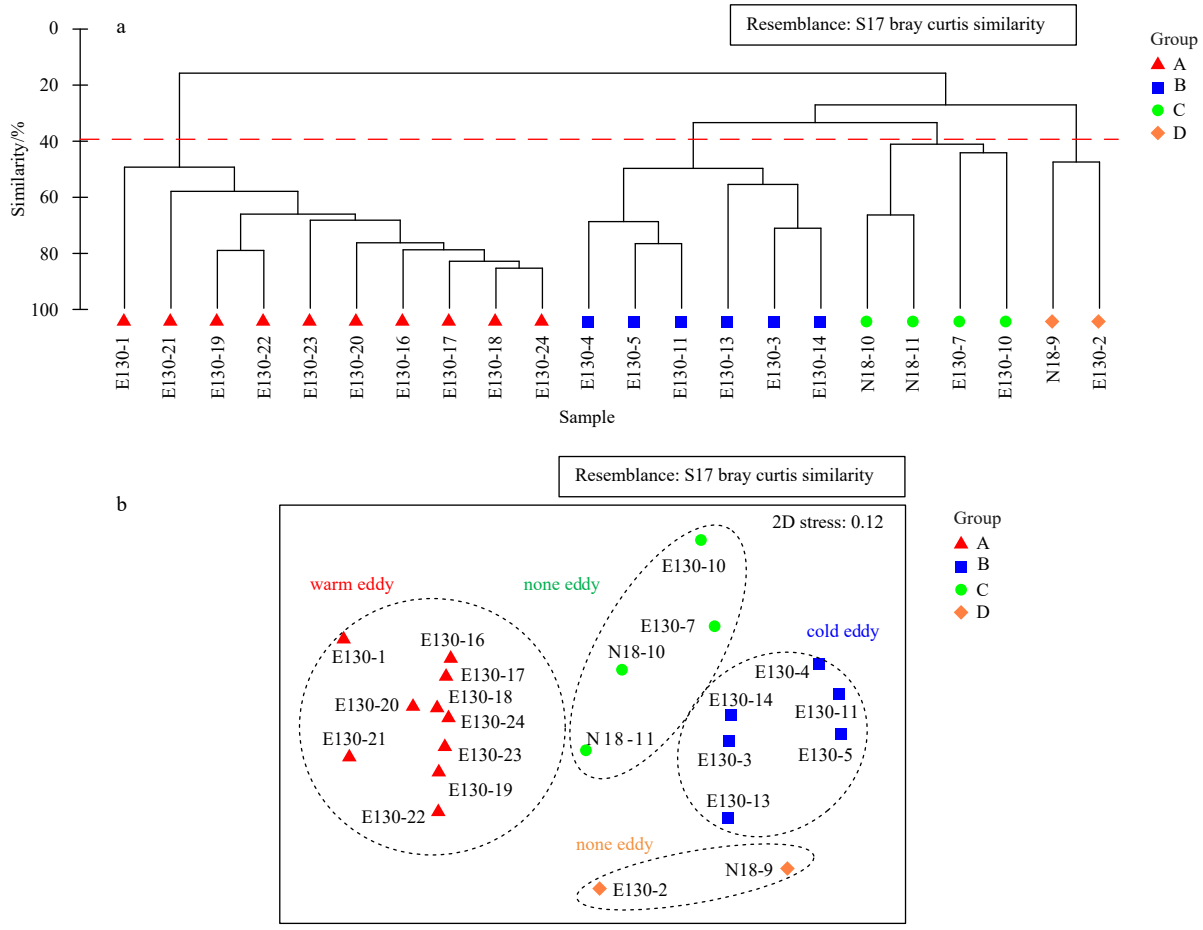

Fig. 10. All stations clustered by Bray-Curtis rank similarities, group average linkage and MDS ordination. a. Group average linkage, and b. MDS ordination.

scale eddies. Accordingly, LCs were less abundant here. Group D covered only two stations which were represented by *U. tenuis*. In general, this study speculated that nutrient availability affected by mesoscale eddies had great impact on the community and distribution of LCs.

4 Discussion

4.1 *Coccolithophore distribution and ecological preference*

Generally, the α-diversity indices were low, indicating the absolute dominance of several species such as *G. oceanica*, *F. profunda* and *E. huxleyi*. Both coccospheres and coccoliths of *G. oceanica* were predominant in this study. This finding was in accordance with previous research in the Pacific Ocean reported by Houghton and Guptha (1991), where *G. oceanica* is the most abundant coccolithophore (mean 57%) under the high-fertility equatorial water mass. *Gephyrocapsa oceanica* prefers waters with temperature between 12°C and 30°C (Okada and McIntyre, 1977; Winter, 1982). In contrast to *G. oceanica*, *E. huxleyi* is a cosmopolitan species thriving in tropical to subpolar waters, and it has a high tolerance of temperature (2°C to 30°C) and salinity (16 to 45) (Hagino et al., 2005). Paasche (1968) and Brand (1982) documented that the optimum temperature of it was 18–24°C, and it never accounts for over 30% of the whole coccolithophore community in warm waters (Cortés et al., 2001). As a consequence, high temperature resulted in the dominance of *G. oceanica* in the WPWP, while it limited the growth of *E. huxleyi*. In addition, coccolithophores also showed diverse vertical distributions. For instance, *G. oceanica* and *E. huxleyi* dominated in the upper euphotic zone, whereas *F. profunda, G. flabellatus* and *A. robusta* commonly occurred in lower photic zone. This is because that they can live in low light condition (less than 1%–4% of the surface irradiance) (Baumann et al., 2005). *Florisphaera profunda* is a biological indicator of nutricline depth and occurs in low nutrient waters (Molfino and McIntyre, 1990). But in this study, *F. profunda* mainly thrived around cold-eddy area and concentrated in DCM layer (Fig. 6c). This is because they were transportated by water masses or upwellings from depths or somewhere and this study considers it has little to do with nutrients. *Umbellosphaera irregularis* and *U. tenuis* were primarily distributed in the upper photic zone of the Pacific oligotrophic waters. Therefore, high abundance of *U. tenuis* was observed at Section A due to the oligotrophic water of KC. Generally, the current coccolithophore community can be characterized into three ecological niches (upper-water adapted, DCM-water adapted, lower-water adapted) as seen from their vertical profiles.

Based on Redfield ratio (N:P = 16:1), phosphorus limitation occurred at Section A (N/P>20) and nitrogen limitation was found at Section B (N/P<14). There were rare studies about the importance of N/P for LCs previously, expect for *E. huxleyi*. Both high N/P and low N/P were found when *E. huxleyi* bloomed (Marañón and González, 1997; Zondervan, 2007). Cortés et al.

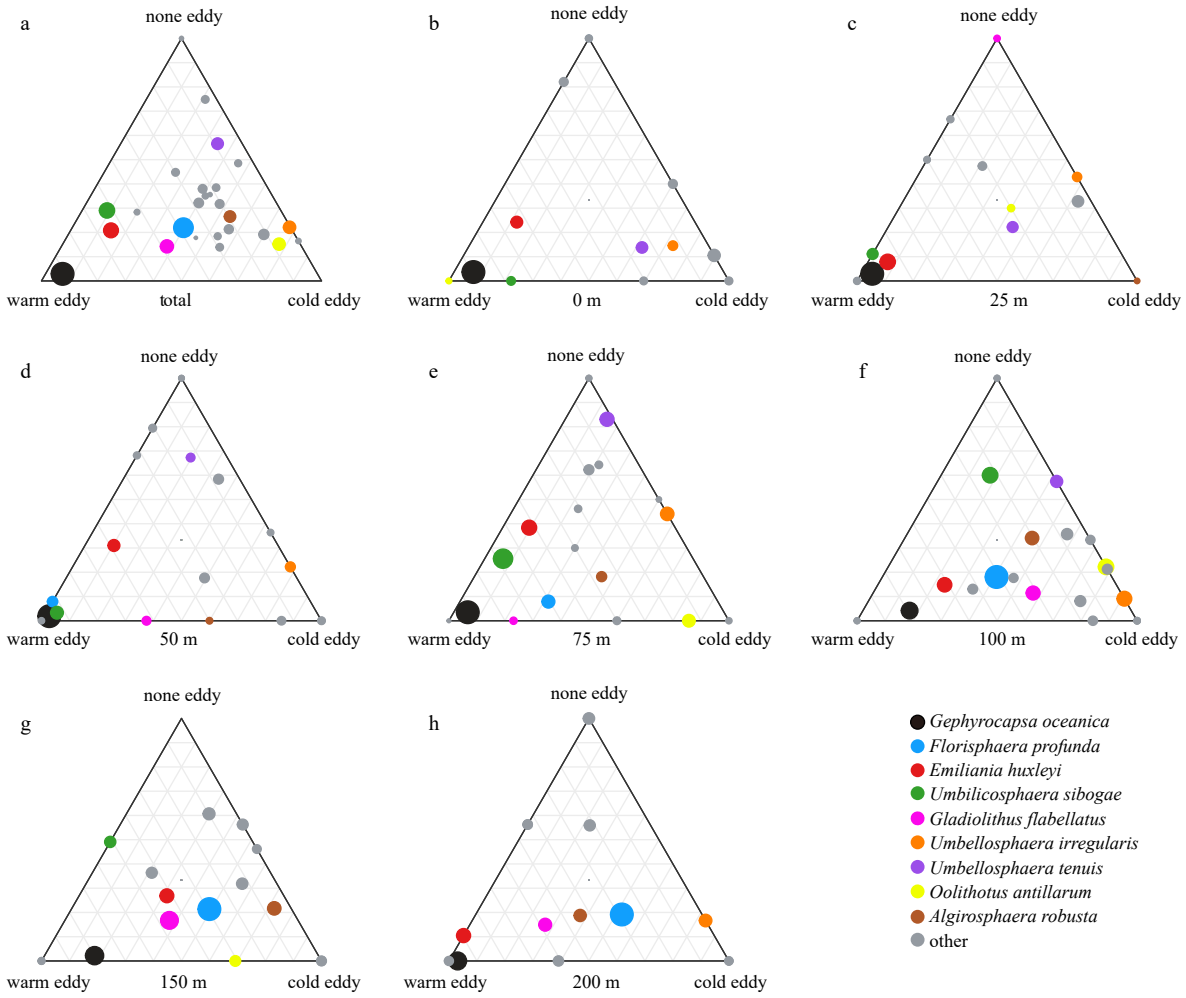

Fig. 11. Ternary plots depicting distribution of the top 9 coccospheres among three different groups: warm eddy, cold eddy and none eddy. a. A ternary plot of integrated-abundance including 7 layers showing the overall distribution of coccospheres of 24 stations. b–h. The composition and distribution of coccospheres at 0 m, 25 m, 50 m, 75 m, 100 m, 150 m and 200 m layer, respectively. Each circle represents one individual coccosphere. The size and position of the circle reflects the relative abundance and the contribution of the indicated compartment to the relative abundance. To distinguish the differentiation among varies groups, Station E130-1 which has ambiguous sectionalization based on hierarchical clustering analysis and multi-dimensional scaling analysis was excluded in the ternary plots.

(2001) reported that the highest density of *E. huxleyi* was observed in relatively high nitrate, while *U. irregularis* was predominant (>50%) at low nitrate condition. At Section B, the abundance of coccospheres and coccoliths both peaked at 2°–5°N under the influences of HE (Figs 6 and A5). High abundances of *E. huxleyi* and *G. oceanica* were also observed near ME because of the nutrients upwelling. In summary, four ecological niches were occupied by coccolithophores according to Young (1994) and Balch (2018): (1) *E. huxleyi*, *G. oceanica*, *U. sibogae* and *O. fragilis* belonging to placolith-bearing and bloom-forming species, which mostly occur in upwelling and coastal area at low or high latitudes; (2) *F. profunda* belonging to floriform species, which are commonly seen in deep water at low to middle latitudes and indicate a well-stratified and stable water system; (3)*U. irregularis* and *U. tenuis* belonging to umbelliform species, which occur in the upper 100 m in oligotrophic waters at subtropical latitudes; and (4) others that make up 80% of species but less than 20% of total abundance.

4.2 *Relationship between LC abundance and environmental factors*

Coccolithophore community was distinguished along mesoscale eddy (Figs 10 and 11). Species richness was similar among warm-eddy, cold-eddy and non-eddy regions, while coccolithophore abundance was prominently different in these regions (p<0.05). This study analyzed the ratios of average LCs abundance in each region to the total of average LCs abundance in three regions. Coccolithophores in warm-eddy region were the biggest contributor (56%) to total LC abundance in the surveyed area, and the abundances were relatively low in cold-eddy region and non-eddy region, accounting for 26% and 17% of the total LC abundance in three regions, respectively. Specifically, the growth of coccolithophores are generally influenced by change in temperature, salinity, dissolved nutrients, concentration of CO_2, depth of mixed layer and other numerous factors (Chen et al., 2007). CCA was applied for the top 8 dominant species of coccospheres and 9 environmental factors (Fig. 12). Results showed that the abundance of LCs was mainly controlled by

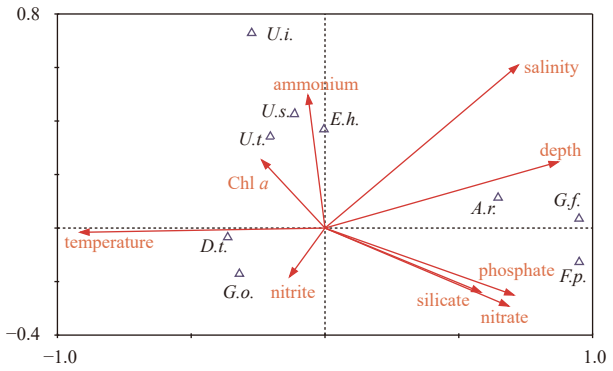

Fig. 12. Results of the canonical correspondence analysis of coccosphere abundance vs. environmental factors (Chl *a*: chlorophyll *a*; *E.h.*: *Emiliania huxleyi*; *A.r.*: *Algirosphaera robusta*; *G.f.*: *Gladiolithus flabellatus*; *F.p.*: *Florisphaera profunda*; *G.o.*: *Gephyrocapsa oceanica*; *D.t.*: *Discosphaera tubifera*; *U.t.*: *Umbellosphaera tenuis*; *U.s.*: *Umbilicosphaera sibogae*).

temperature, salinity, sampling depth and a group of nutrients (including nitrate, phosphate, silicate and ammonium). Axis 1 was observed to be ammonium dependent, while Axis 2 was positively related to depth and concentration of phosphate but negatively related to temperature. Therefore, this study confirmed that coccolithophore species are influenced by environmental variables at different degrees.

Both *G. flabellatus a*nd *A. robusta* were deep-water species, thus they were deeply affected by sampling depth. Light intensity could be the limiting factor for them. On the contrary, *D. tubifera* and *G. oceanica*, the two species mostly observed in the upper euphotic layer, showed negative correlation to sampling depth and salinity, indicating their preference for high light and low salinity conditions. Positive correlation was observed between water temperature, and the abundance of *D. tubifera* and *G. oceanica*, but negative correlation was found between water temperature and the abundance of *A. robusta* and *G. flabellatus*. However, temperature showed no influence on *E. huxleyi*, which was a broadly widespread species (Houghton and Guptha, 1991). In our CCA analysis, *E. huxleyi*, *D. tubifera* and *U. tenuis* were positively correlated with the ammonium concentration. Sufficient nutrients such as nitrate and phosphate favored the growth of *F. profunda*. As per literature, nitrogen plays an essential role in protein synthesis and cellular biomass accumulation and phosphate reflects the N/P rather than absolute availability of key macronutrients (Müller et al., 2017). This study also found that coccolithophore abundance variation were strongly dependent on silicate concentration (Fig. 12). Recent findings showed that silicon is required in calcification of certain coccolithophore species (Durak et al., 2016). For example, *Prymnesium neolepis*, formerly known as *Hyalolithus neolepis*, requires silicon because it forms silicic rather than calcite coccoliths. For other species producing calcite, such as *C. braarudii* and *C. leptoporus*, low concentration of silicate (<2 μmol/L) was growth-inhibiting and teratogenic (Thamatrakoln and Hildebrand, 2008).

4.3 *Estimate of coccolithophore PIC and POC*

Coccolithophores are regarded as a group of calcifiers, because they can produce and excrete calcite scales that cover the cells or fall off as detached coccoliths (Balch, 2018). In this study, the relative contribution of *G. oceanica* to coccolithophore PIC was higher than that of any other species (up to 30%), which was different from that in the South China Sea (the relative contribution of *Gephyrocapsa* spp., *E. huxleyi* and *F. profunda* to water column calcite was 8%, 13% and 29%, respectively) (Jin et al., 2016). The discrepancy in relative contribution was caused by the different relative abundance of *G. oceanica* in the study region and the South China Sea. Although *U. sibogae* and *O. fragilis* were not abundant (Table 2), they contributed significantly (26.1% and 18.5%, respectively) to global calcite inventory (Fig. 8a) due to the large coccolith calcite (16.9 pg and 96.8 pg calcite for a coccolith of *U. sibogae* and *O. fragilis* at mean length). The surface distribution of POC was in accordance with the abundance of coccospheres. The distribution trend of depth-integral and surface POC were similar to that of LCs (Fig. 9). Within this study, the biomass values (mean 0.14 μg/L (according to carbon), median 0.05 μg/L (according to carbon), maximum 1.88 μg/L (according to carbon)) were in accordance with previous observations, and the estimated biomass were lower than 5 μg/L (according to carbon) between the equator and 40°N (O'Brien et al., 2013). However, these low biomass may be caused by the oligotrophic waters in the WPWP. Highest biomass were recorded in the North Atlantic (mean 1.7 μg/L (according to carbon), median 0.12 μg/L (according to carbon), maximum 127.2 μg/L (according to carbon)) and lowest were observed in the Pacific Ocean (mean 0.30 μg/L (according to carbon), median 0.04 μg/L (according to carbon), maximum 20.0 μg/L (according to carbon)) (O'Brien et al., 2013). Biomass peaked around 60°N and 20°–40°S, and declined towards both the poles and the equator. However, the calcite mass was underestimated without *G. flabellatus* and *O. antillarum*, and the biovolumes were overestimated with coccosphere diameter rather than cytoplasm. Thus, PIC/POC may be undervalued in this study. This ratio is considered as a relative strength index between photosynthesis and calcification, indirectly reflecting the ecological role of coccolithophores in global carbon cycle.

5 Conclusions

The present study carried out field study on coccolithophore community structure, species abundance and their relationship with physical background (mainly mesoscale eddies) in the western Pacific Ocean. The whole coccolithophore populations were dominated by *G. oceanica*, *F. profunda*, *E. huxleyi*, *U. sibogae*, *G. flabellatus* and *U. tenuis*. Based on cell abundance and biovolume information, this study estimated coccolithophore calcite standing stocks and discussed their potential contribution to sediment flux. This study identified three ecological niche traits among coccolithophore community in the study area. Coccolithophore community structure and diversity were significantly different among warm-eddy region, cold-eddy region and non-eddy region. The ratios of average LC abundance in each region to the total of average LC abundance in three regions were 56%, 26%, and 17%, respectively. This field study widened the current dataset of coccolithophores in the western Pacific Ocean and could be incorporated into regional biogeochemical models with the scenarios of ongoing and future climate change.

Acknowledgements

We thank Dongliang Yuan from the Institute of Oceanology of Chinese Academy of Sciences for providing hydrographic (CTD) data. We gratefully acknowledge the crew of the R/V *Kexue* for their assistance and all the participants for their input and contributions during the cruise. We also thank the Open Cruise Project in the western Pacific Ocean of National Nature Science Foundation of China (NORC2017-09) for sharing their ship time.

References

Arruda W Z, Nof D. 2003. The Mindanao and Halmahera eddies—twin eddies induced by nonlinearities. Journal of Physical Oceanography, 33(12): 2815–2830, doi: 10.1175/1520-0485(2003)033<2815:TMAHEE>2.0.CO;2

Balch W M. 2018. The ecology, biogeochemistry, and optical properties of coccolithophores. Annual Review of Marine Science, 10: 71–98, doi: 10.1146/annurev-marine-121916-063319

Baumann K H, Andruleit H, Böckel B, et al. 2005. The significance of extant coccolithophores as indicators of ocean water masses, surface water temperature, and palaeoproductivity: a review. Paläontologische Zeitschrift, 79(1): 93–112

Berger W H. 1976. Treatise on Chemical Oceanography. London: Academic Press, 265–388

Bollmann J, Cortés M Y, Haidar A T, et al. 2002. Techniques for quantitative analyses of calcareous marine phytoplankton. Marine Micropaleontology, 44(3–4): 163–185

Brand L E. 1982. Genetic variability and spatial patterns of genetic differentiation in the reproductive rates of the marine coccolithophores *Emiliania huxleyi* and *Gephyrocapsa oceanica*. Limnology and Oceanography, 27(2): 236–245, doi: 10.4319/lo.1982.27.2.0236

Brzezinski M A, Nelson D M. 1986. A solvent extraction method for the colorimetric determination of nanomolar concentrations of silicic acid in seawater. Marine Chemistry, 19(2): 139–151, doi: 10.1016/0304-4203(86)90045-9

Chen Yuh-Ling, Chen Houng-Yung, Chung Cheng-Wei. 2007. Seasonal variability of coccolithophore abundance and assemblage in the northern South China Sea. Deep-Sea Research Part II: Topical Studies in Oceanography, 54(14–15): 1617–1633

Chen Yunyan, Sun Xiaoxia, Zhu Mingliang, et al. 2017. Spatial variability of phytoplankton in the Pacific western boundary currents during summer 2014. Marine and Freshwater Research, 68(10): 1887–1900, doi: 10.1071/MF16297

Chen Yunyan, Sun Xiaoxia, Zhu Mingliang. 2018. Net-phytoplankton communities in the Western Boundary Currents and their environmental correlations. Journal of Oceanology and Limnology, 36(2): 305–316, doi: 10.1007/s00343-017-6261-8

Clarke K R, Gorley R N, Somerfield P, et al. 2014. Change in Marine Communities: An Approach to Statistical Analysis and Interpretation. 3rd ed. Plymouth, UK: Primer-E

Cortés M Y, Bollmann J, Thierstein H R. 2001. Coccolithophore ecology at the HOT station ALOHA, Hawaii. Deep-Sea Research Part II: Topical Studies in Oceanography, 48(8–9): 1957–1981

Cox M A, Cox T. 1992. Interpretation of Stress in non-metric multidimensional scaling. Statistica Applicata, 4(4): 611–618

Doney S C, Fabry V J, Feely R A, et al. 2009. Ocean acidification: the other CO_2 problem. Annual Review of Marine Science, 1: 169–192, doi: 10.1146/annurev.marine.010908.163834

Durak G M, Taylor A R, Walker C E, et al. 2016. A role for diatom-like silicon transporters in calcifying coccolithophores. Nature Communications, 7(1): 10543, doi: 10.1038/ncomms10543

Eppley R W, Reid F M H, Strickland J D H. 1970. Estimates of phytoplankton crop size, growth rate, and primary production. In: Strickland J D H, ed. The Ecology of the Plankton off La Jolla, California, in the Period April Through September 1967. California: University of California

Frada M, Young J, Cachão M, et al. 2010. A guide to extant coccolithophores (Calcihaptophycidae, Haptophyta) using light microscopy. Journal of Nannoplankton Research, 31(2): 58–112

Guo Shujin, Feng Yuanyuan, Wang Lei, et al. 2014. Seasonal variation in the phytoplankton community of a continental-shelf sea: the East China Sea. Marine Ecology Progress Series, 516: 103–126, doi: 10.3354/meps10952

Hagino K, Okada H, Matsuoka H. 2000. Spatial dynamics of coccolithophore assemblages in the Equatorial Western-Central Pacific Ocean. Marine Micropaleontology, 39(1–4): 53–72

Hagino K, Okada H, Matsuoka H. 2005. Coccolithophore assemblages and morphotypes of *Emiliania huxleyi* in the boundary zone between the cold Oyashio and warm Kuroshio currents off the coast of Japan. Marine Micropaleontology, 55(1–2): 19–47

Honjo S. 1996. Fluxes of particles to the interior of the open oceans. In: Ittekkot V, Schafer P, Honjo S, et al., eds. Particle Flux in the Ocean. Chichester: Wiley, 91–154

Honjo S, Okada H. 1974. Community structure of coccolithophores in the photic layer of the mid-pacific. Micropaleontology, 20(2): 209–230, doi: 10.2307/1485061

Houghton S D, Guptha M V S. 1991. Monsoonal and fertility controls on Recent marginal sea and continental shelf coccolith assemblages from the western Pacific and northern Indian oceans. Marine Geology, 97(3–4): 251–259

Hu Dunxin, Wu Lixin, Cai Wenju, et al. 2015. Pacific western boundary currents and their roles in climate. Nature, 522(7556): 299–308, doi: 10.1038/nature14504

Hu Shijian, Hu Dunxin, Guan Cong, et al. 2016. Interannual variability of the mindanao current/undercurrent in direct observations and numerical simulations. Journal of Physical Oceanography, 46(2): 483–499, doi: 10.1175/JPO-D-15-0092.1

Hutchins D A. 2011. Oceanography: forecasting the rain ratio. Nature, 476(7358): 41–42

Jiang Bo, Wu Xinrong, Ding Jie, et al. 2016. Comparison on the methods of determining the depths of thermocline in the South China Sea. Marine Science Bulletin (in Chinese), 35(1): 64–73

Jin Xiaobo, Liu Chuanlian, Poulton A J, et al. 2016. Coccolithophore responses to environmental variability in the South China Sea: species composition and calcite content. Biogeosciences, 13(16): 4843–4861, doi: 10.5194/bg-13-4843-2016

Jordan R W, Cros L, Young J R. 2004. A revised classification scheme for living haptophytes. Micropaleontology, 50(S1): 55–79

Karl D M, Tien G. 1992. Magic: a sensitive and precise method for measuring dissolved phosphorus in aquatic environments. Limnology and Oceanography, 37(1): 105–116, doi: 10.4319/lo.1992.37.1.0105

Li Xiaofan, Sui C H, Adamec D, et al. 1998. Impacts of precipitation in the upper ocean in the western Pacific warm pool during TOGA-COARE. Journal of Geophysical Research: Oceans, 103(C3): 5347–5359, doi: 10.1029/97JC03420

Liu Haijiao, Sun Jun, Wang Dongxiao, et al. 2018. Distribution of living coccolithophores in eastern Indian Ocean during spring intermonsoon. Scientific Reports, 8(1): 12488, doi: 10.1038/s41598-018-29688-w

Liu Haijiao, Xue Bing, Feng Yuanyuan, et al. 2015. Size-fractionated Chlorophyll *a* biomass in the northern South China Sea in summer 2014. Chinese Journal of Oceanology and Limnology, 34(4): 672–682

López-Fuerte F O, Gárate-Lizárraga I, Siqueiros-Beltrones D A, et al. 2015. First record and geographic range extension of the coccolithophore *Scyphosphaera apsteinii* Lohman, 1902 (Haptophyta: Pontosphaeraceae) from the Pacific coast of Mexico. Check List, 11(5): 1–3

Marañón E, González N. 1997. Primary production, calcification and macromolecular synthesis in a bloom of the coccolithophore *Emiliania huxleyi* in the North Sea. Marine Ecology Progress Series, 157: 61–77, doi: 10.3354/meps157061

Messié M, Radenac M H. 2006. Seasonal variability of the surface chlorophyll in the western tropical Pacific from SeaWiFS data. Deep-Sea Research Part I: Oceanographic Research Papers, 53(10): 1581–1600, doi: 10.1016/j.dsr.2006.06.007

Molfino B, McIntyre A. 1990. Nutricline variation in the equatorial Atlantic coincident with the Younger Dryas. Paleoceanography, 5(6): 997–1008, doi: 10.1029/PA005i006p00997

Müller M N, Trull T W, Hallegraeff G M. 2017. Independence of nutrient limitation and carbon dioxide impacts on the Southern Ocean coccolithophore *Emiliania huxleyi*. The ISME Journal, 11(8): 1777–1787, doi: 10.1038/ismej.2017.53

O'Brien C J, Peloquin J A, Vogt M, et al. 2013. Global marine plankton functional type biomass distributions: coccolithophores. Earth System Science Data, 5(2): 259–276, doi: 10.5194/essd-5-259-2013

Okada H, Honjo S. 1973. The distribution of oceanic coccolithophorids in the Pacific. Deep Sea Research and Oceanographic Ab-

stracts, 20(4): 355–374, doi: 10.1016/0011-7471(73)90059-4
Okada H, Honjo S. 1975. Distribution of coccolithophores in marginal seas along the western Pacific Ocean and in the Red Sea. Marine Biology, 31(3): 271–285, doi: 10.1007/BF00387154
Okada H, McIntyre A. 1977. Modern coccolithophores of the Pacific and north atlantic oceans. Micropaleontology, 23(1): 1–55, doi: 10.2307/1485309
Paasche E. 1968. Marine plankton algae grown with light-dark cycles. II. *Ditylum brightwellii* and *Nitzschia turgidula*. Physiologia Plantarum, 21(1): 66–77, doi: 10.1111/j.1399-3054.1968.tb07231.x
Pai S C, Tsau Y J, Yang T I. 2001. pH and buffering capacity problems involved in the determination of ammonia in saline water using the indophenol blue spectrophotometric method. Analytica Chimica Acta, 434(2): 209–216, doi: 10.1016/S0003-2670(01)00851-0
Painter S C, Poulton A J, Allen J T, et al. 2010. The COPAS'08 expedition to the Patagonian Shelf: physical and environmental conditions during the 2008 coccolithophore bloom. Continental Shelf Research, 30(18): 1907–1923, doi: 10.1016/j.csr.2010.08.013
Perrin L, Probert I, Langer G, et al. 2016. Growth of the coccolithophore *Emiliania huxleyi* in light- and nutrient-limited batch reactors: relevance for the BIOSOPE deep ecological niche of coccolithophores. Biogeosciences, 13(21): 5983–6001, doi: 10.5194/bg-13-5983-2016
R Core Team. 2013. R: a language and environment for statistical computing. Vienna, Austria: R Foundation for Statistical Computing
Reid F M H. 1980. Coccolithophorids of the North Pacific Central Gyre with notes on their vertical and seasonal distribution. Micropaleontology, 26(2): 151–176, doi: 10.2307/1485436
Saavedra-Pellitero M, Baumann K H, Flores J A, et al. 2014. Biogeographic distribution of living coccolithophores in the Pacific sector of the Southern Ocean. Marine Micropaleontology, 109: 1–20, doi: 10.1016/j.marmicro.2014.03.003
Saavedra-Pellitero M, Flores J A, Lamy F, et al. 2011. Coccolithophore estimates of paleotemperature and paleoproductivity changes in the southeast Pacific over the past ~ 27 kyr. Paleoceanography, 26(1): PA1201
Shutler J D, Land P E, Brown C W, et al. 2013. Coccolithophore surface distributions in the North Atlantic and their modulation of the air-sea flux of CO_2 from 10 years of satellite Earth observation data. Biogeosciences, 10(4): 2699–2709, doi: 10.5194/bg-10-2699-2013
Sun Jun. 2007. Organic carbon pump and carbonate counter pump of living coccolithophorid. Advances in Earth Science (in Chinese), 22(12): 1231–1239
Sun Jun, An Baizheng, Dai Minhan, et al. 2011. Living coccolithophores in the Western South China sea in summer 2007. Oceanologia et Limnologia Sinica (in Chinese), 42(2): 170–178
Sun Jun, Gu Xiaoyao, Feng Yuanyuan, et al. 2014. Summer and winter living coccolithophores in the Yellow Sea and the East China Sea. Biogeosciences, 11(3): 779–806, doi: 10.5194/bg-11-779-2014
Sun Jun, Liu Dongyan. 2003. Geometric models for calculating cell biovolume and surface area for phytoplankton. Journal of Plankton Research, 25(11): 1331–1346, doi: 10.1093/plankt/fbg096
Sun Jun, Liu Dongyan, Ning Xiuren. 2003. Phytoplankton in the Prydz Bay and the adjacent Indian sector of the Southern Ocean during the austral summer 2001/2002. Oceanologia et Limnologia Sinica (in Chinese), 34(5): 519–532
Taylor A R, Brownlee C, Wheeler G. 2017. Coccolithophore cell biology: chalking up progress. Annual Review of Marine Science, 9: 283–310, doi: 10.1146/annurev-marine-122414-034032
ter Braak C J F. 1986. Canonical correspondence analysis: a new eigenvector technique for multivariate direct gradient analysis. Ecology, 67(5): 1167–1179, doi: 10.2307/1938672
Thamatrakoln K, Hildebrand M. 2008. Silicon uptake in diatoms revisited: a model for saturable and nonsaturable uptake kinetics and the role of silicon transporters. Plant Physiology, 146(3): 1397–1407, doi: 10.1104/pp.107.107094
Wei Yuqiu, Liu Haijiao, Zhang Xiaodong, et al. 2017. Physicochemical conditions in affecting the distribution of spring phytoplankton community. Chinese Journal of Oceanology and Limnology, 35(6): 1342–1361, doi: 10.1007/s00343-017-6190-6
Wei Yuqiu, Zhang Guicheng, Chen Ju, et al. 2019. Dynamic responses of picophytoplankton to physicochemical variation in the eastern Indian Ocean. Ecology and Evolution, 9(8): 5003–5017, doi: 10.1002/ece3.5107
Welschmeyer N A. 1994. Fluorometric analysis of chlorophyll *a* in the presence of chlorophyll *b* and pheopigments. Limnology and Oceanography, 39(8): 1985–1992, doi: 10.4319/lo.1994.39.8.1985
Winter A. 1982. Paleoenvironmental interpretation of Quaternary coccolith assemblages from the Gulf of Aqaba (Elat), Red Sea. Revista Española de Micropaleontologia, 14: 291–314
Yang Tiennan, Wei Kuoyen. 2003. How many coccoliths are there in a coccosphere of the extant coccolithophorids?—A compilation. Journal of Nannoplankton Research, 25(1): 7–15
Yang Tiennan, Wei Kuoyen, Chen Liling. 2003. Occurrence of coccolithophorids in the northeastern and central South China Sea. Taiwania, 48(1): 29–45
Young J. 1994. Functions of coccoliths. In: Winter A, Siesser W G, eds. Coccolithophores. Cambridge, UK: Cambridge University Press, 63–82
Young J R, Ziveri P. 2000. Calculation of coccolith volume and it use in calibration of carbonate flux estimates. Deep-Sea Research Part II: Topical Studies in Oceanography, 47(9–11): 1679–1700
Zhai Fangguo, Hu Dunxin, Wang Qingye. 2013. Study on the seasonal variability of the Halmahera Eddy. Marine Sciences (in Chinese), 37(11): 85–94
Zondervan I. 2007. The effects of light, macronutrients, trace metals and CO_2 on the production of calcium carbonate and organic carbon in coccolithophores—A review. Deep-Sea Research Part II: Topical Studies in Oceanography, 54(5–7): 521–537

Appendix:

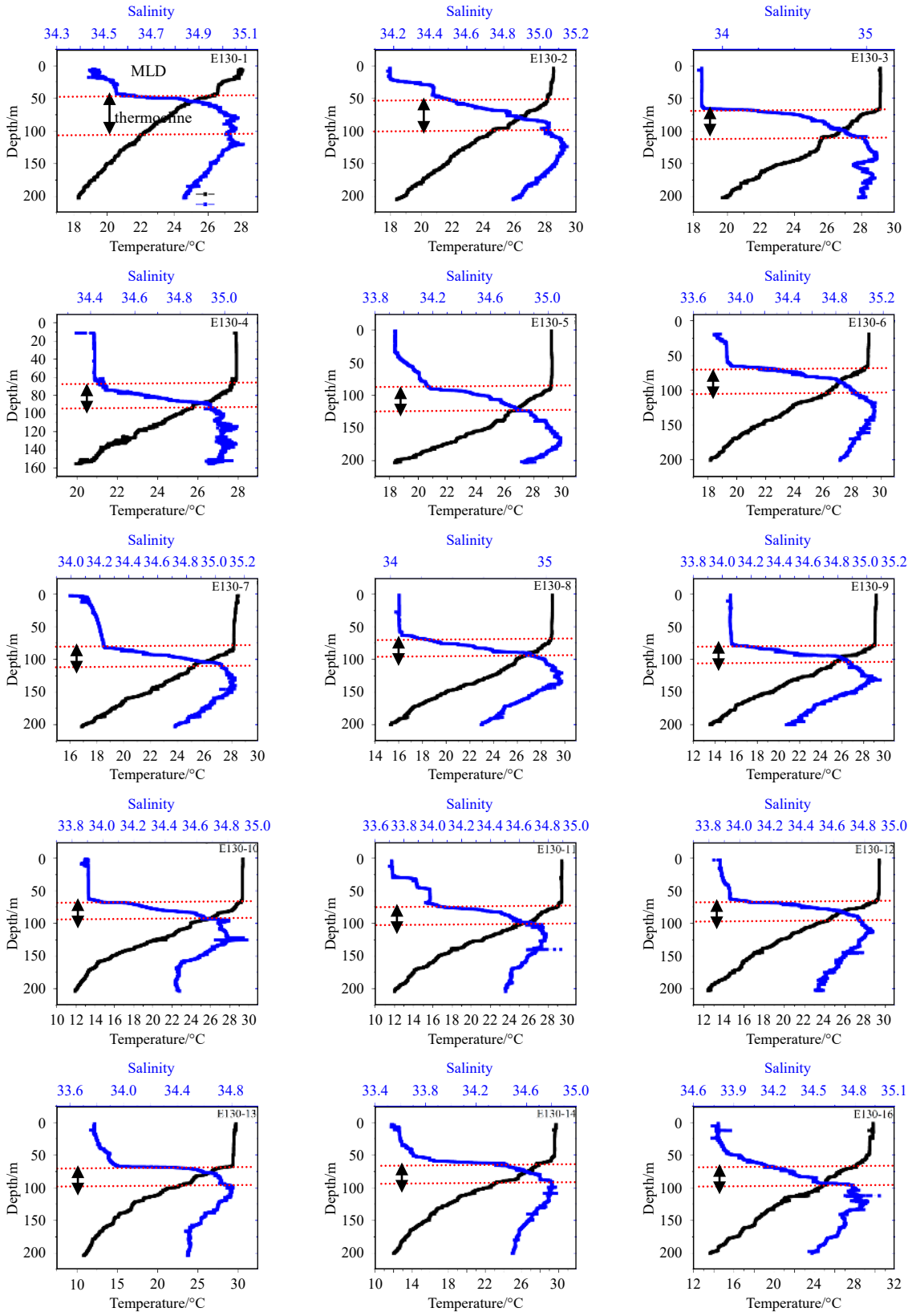

Fig. A1.

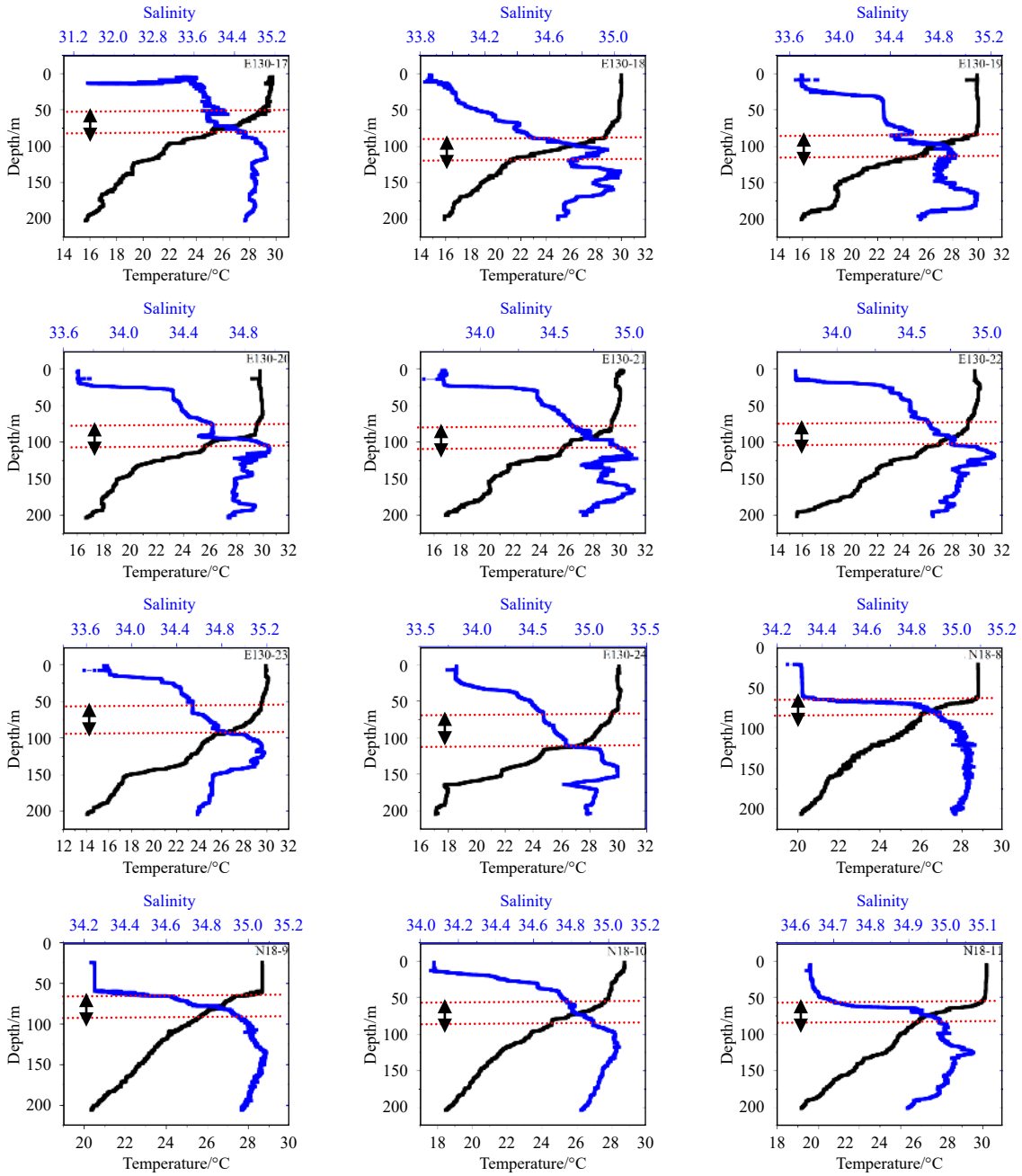

Fig. A1. Vertical profiles of temperature and salinity along 27 stations showing mixed layer depth (MLD) and thermocline depth.

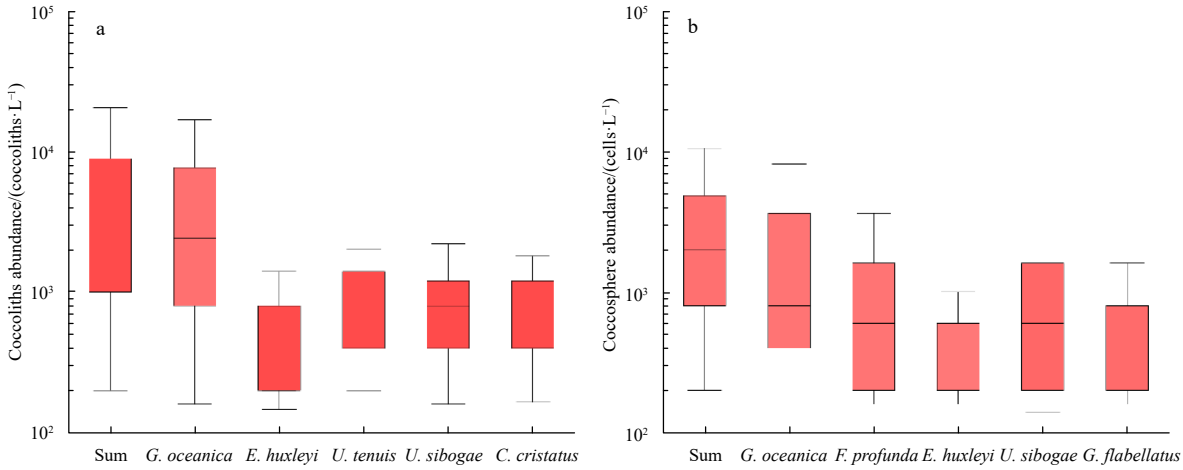

Fig. A2. The abundance of dominant coccolithophore species in the western Pacific Ocean.

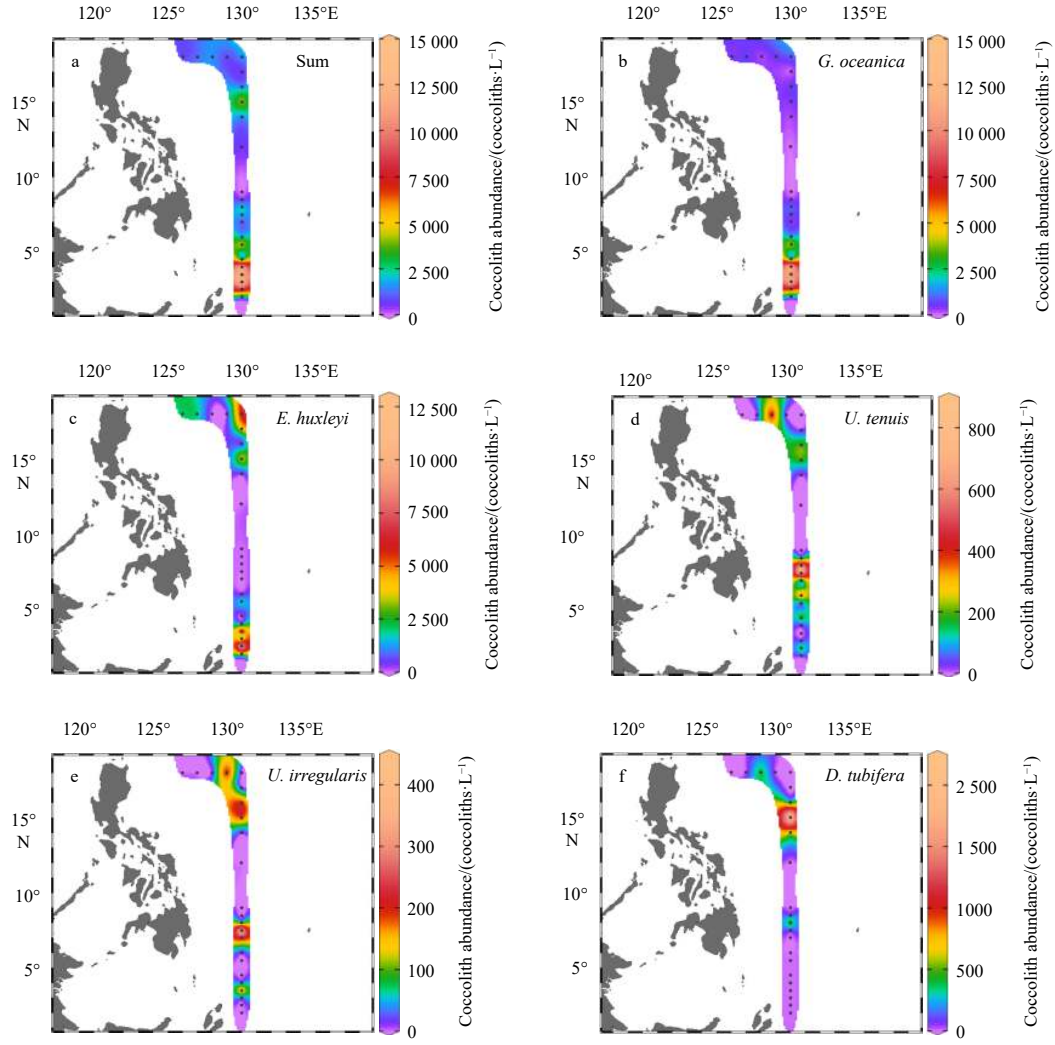

Fig. A3. Surface distribution of dominant coccoliths in the surveyed area.

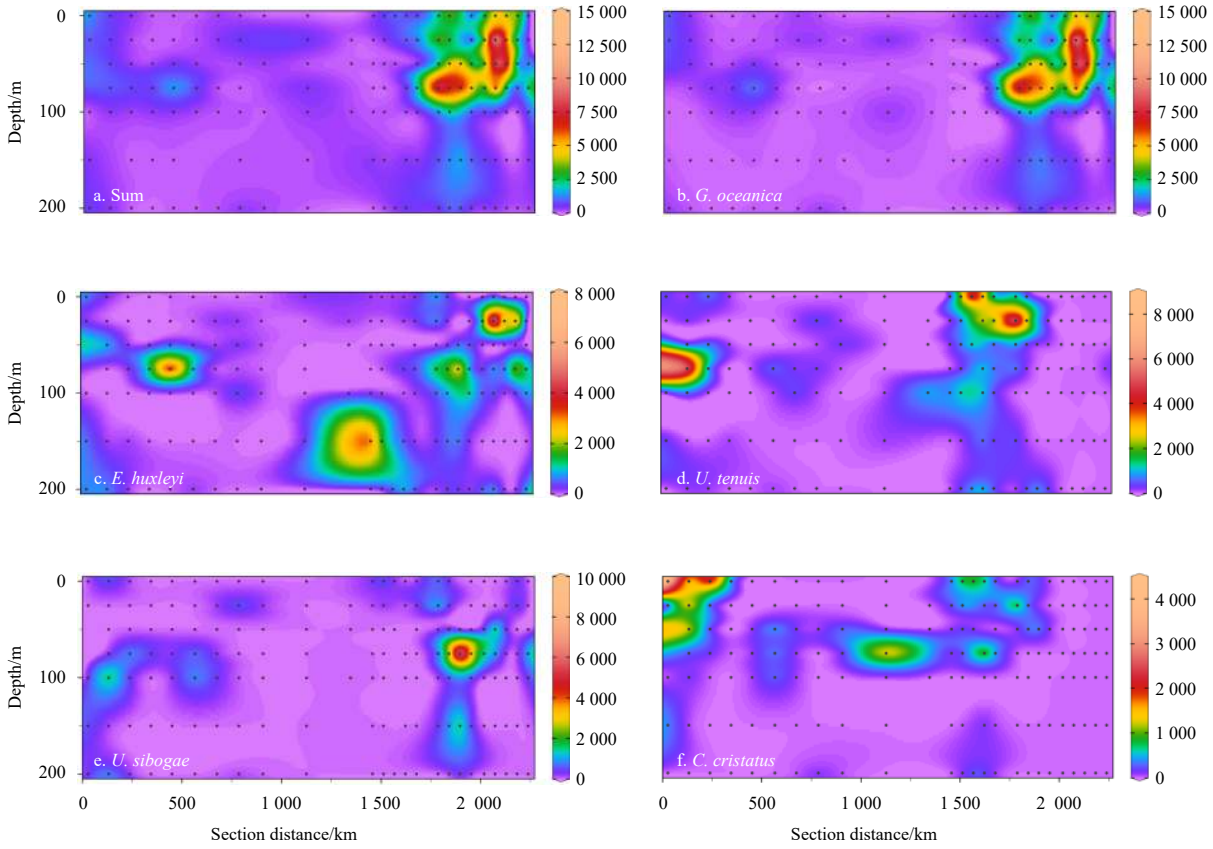

Fig. A4. Dominant coccolith distributions (coccoliths/L) along section of the surveyed area.

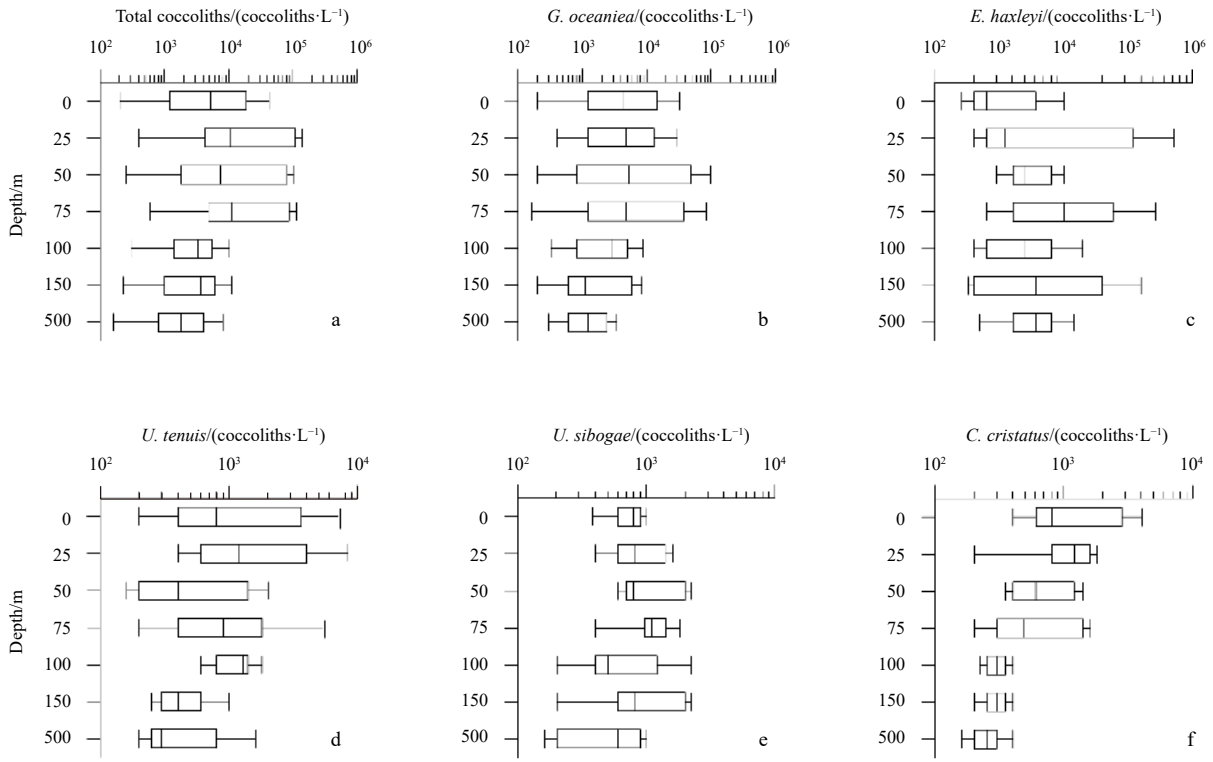

Fig. A5. Vertical distributions of dominant coccoliths in the surveyed area.

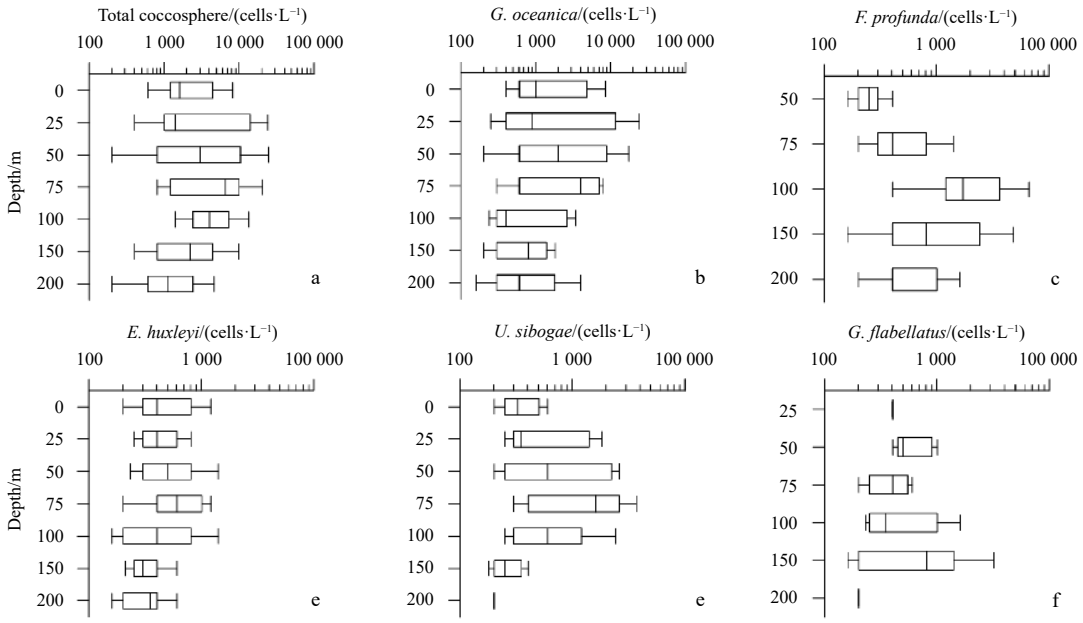

Fig. A6. Vertical distributions of dominant coccospheres in the surveyed area.

Table A1. Overview of α-biodiversity indices in the water column of survey area

Index	Depth/m						
	0	25	50	75	100	150	200
Richness	0–10 (3.1)	1–6 (3.5)	1–11 (3.9)	1–14 (6)	2–11 (5.7)	1–10 (4.1)	1–9 (3.1)
Shannon	0–2.7 (1.1)	0–2.2 (1.3)	0–3.3 (1.3)	0–3 (1.7)	0.5–2.9 (1.7)	0–3.1 (1.4)	0–2.9 (1.2)
Simpon	0–1 (0.5)	0–0.8 (0.5)	0–0.9 (0.5)	0–0.9 (0.6)	0.2–0.8 (0.6)	0–0.9 (0.5)	0–0.9 (0.4)
Chao1	0–10 (3.1)	1–6 (3.5)	1–11 (3.9)	1–14 (6)	2–11 (5.7)	1–10 (4.1)	1–9 (3.1)

Note: The value in parenthesis are the mean value.